MINOS results from the NuMI beam

Žarko Pavlović and MINOS collaboration

Citation: AIP Conference Proceedings **981**, 18 (2008); doi: 10.1063/1.2898928
View online: http://dx.doi.org/10.1063/1.2898928
View Table of Contents: http://scitation.aip.org/content/aip/proceeding/aipcp/981?ver=pdfcov
Published by the AIP Publishing

MINOS results from the NuMI beam

Žarko Pavlović (for the MINOS collaboration)

The University of Texas at Austin

Abstract. We present an updated measurement of ν_μ disappearance in the NuMI neutrino beam using MINOS detectors. This preliminary result is based on 2.5×10^{20} protons on target. We observe 563 charged-current ν_μ events in the Far Detector, where we expect 738 ± 30 in the absence of neutrino oscillations. The observed deficit is consistent with oscillation hypothesis. The best fit to oscillation parameters yields $\Delta m^2_{23} = 2.38^{+0.20}_{-0.16} \times 10^{-3} eV^2$ and $\sin^2 2\theta_{23} = 1.00_{-0.08}$ with errors quoted at the 68% confidence level. The uncertainties include both statistical and systematic errors.

Keywords: Neutrino mass and mixing
PACS: 14.60.Pq

1. INTRODUCTION

The MINOS experiment is a long baseline neutrino disappearance experiment designed to study ν_μ disappearance phenomena observed in atmospheric neutrino experiments [1, 2]. The phenomenon was also observed in K2K accelerator experiment [3]. The goal of the MINOS experiment is to verify the $\nu_\mu \rightarrow \nu_\tau$ oscillation hypothesis and to measure precisely the relevant mass splitting Δm^2_{23} and mixing angle $\sin^2 2\theta_{23}$. Additionally, MINOS will look for the appearance of the ν_es in the neutrino beam due to sub-dominant $\nu_\mu \rightarrow \nu_e$ oscillation mode. Depending on the value of θ_{13} MINOS could either make the first measurement or improve the limit on θ_{13}. Details of the ν_e appearance analysis were presented at this workshop by Mayly Sanchez [4].

The neutrinos for MINOS experiment are produced in Fermilab's NuMI beam line. MINOS uses two neutrino detectors to study the neutrino beam at two locations on the beam axis. The Near Detector (ND) is on site at Fermilab, 1km downstream of the production point. It measures the neutrino beam composition and spectrum before neutrino oscillations take place. The Far Detector (FD) is located 735km away in the Soudan mine Minnesota. Comparing the reconstructed neutrino spectrum at the ND and the FD allows the extraction of the oscillation parameters.

We perform the analysis in a two neutrino oscillation framework. Within this framework the probability to observe a ν_μ at the FD if we start with a ν_μ, is given with:

$$P(\nu_\mu \rightarrow \nu_\mu) = 1 - \sin^2(2\theta)\sin^2\left(1.27\frac{\Delta m^2[eV^2]L[km]}{E[GeV]}\right)$$

where L is the distance from the target and E is the neutrino energy. The measured mixing angle θ and mass splitting Δm^2 can be identified as θ_{23} and Δm^2_{23} in the limit where $P(\nu_\mu \rightarrow \nu_e) = 0$.

The first MINOS result [5, 6] was based upon 1.27×10^{20} protons on target. We present here the updated results using 2.50×10^{20} protons on target. The present analysis also incorporates several improvements. We now include the events with E_ν above 30GeV. The FD fiducial volume was expanded by 3.2%. A new track reconstruction algorithm is used, resulting in 4% increase in muon track reconstruction and fitting efficiency. An improved procedure for selecting ν_μ CC signal events and rejecting the NC backgrounds is used, resulting in approximately 1% increase in selection efficiency and better than a factor of two reduction of NC background. Finaly an upgraded neutrino interaction simulation package [9] is used that has a more accurate models of hadronization, intranuclear rescattering and deep inelastic scattering.

2. THE NUMI BEAM

The NuMI beam is a conventional, horn focused neutrino beam providing an intense and almost pure ν_μ beam. The neutrinos are produced using 120GeV protons from the Main Injector and steering them on a 94cm long water cooled segmented graphite target. Before striking the target, the proton beam is bent downward by 58mrad to point to the FD. Protons are delivered in $10\mu s$ spills every 2.4 seconds, with each spill containing up to 4.0×10^{13} protons. The secondary particles produced in proton graphite interactions are focused using two magnetic horns. The horns focus positive particles and defocus negative ones. The focused mesons, mainly pions and kaons, decay while flying through the 675m long evacuated decay pipe. Decays of these mesons give rise to the neutrino beam. The composition of the beam is 92.9% ν_μ, 5.8 % $\bar{\nu}_\mu$ and 1.3% ν_e and $\bar{\nu}_e$.

An important feature of the NuMI beam-line is the

CP981, *9th International Workshop on Neutrino Factories, Superbeams, and Betabeams -NuFact 07,*
edited by O. Yasuda, C. Ohmori, and N. Mondal,

ability to adjust the energy of the neutrino beam. This can be achieved by changing the relative distance between the target and the focusing horns. Pulling the target away from horns results in focusing of the stiffer mesons, while the soft ones miss the horns altogether. Bringing the target closer to horns allows the horns to capture the soft pions and focus them down the decay pipe. Since the neutrino energy is proportional to the parent energy, changing the target position changes the neutrino energy spectrum.

In addition to changing the target position, the horn current can be varied as well. Higher horn currents result in focusing of particles coming from the target with higher transverse momentum. Taking data with various target positions and horn currents thus corresponds to focusing of different regions in the momentum space of pions flying of the target. For oscillation analysis it is favorable to run in a beam configuration that gives the largest flux in lower energy bins. The majority of data was taken in the low energy configuration, however small part of the data was taken in higher energy configurations.

The biggest uncertainty in predicting the neutrino flux comes from the uncertainty in hadron production. We use the data taken in other beam configurations to tune the beam Monte Carlo simulation to better match the ND data. The details of tuning procedure were discussed by Sacha Kopp at this workshop [8].

3. THE NEUTRINO DETECTORS, EVENT RECONSTRUCTION AND SELECTION

The two MINOS detectors are almost identical in design. This allows for the cancellation of the majority of the uncertainties related to modeling of neutrino interactions and detector response. The detectors are steel-scintillator tracking calorimeters built out of planes consisting of 2.54cm thick steel plane and a 1cm thick scintillator plane. Both detectors are magnetized with toroidal magnetic field averaging 1.3T allowing for the reconstruction of the charge through the curvature of the track.

The ND has 282 planes that have irregular $4 \times 6m^2$ octagonal shape. The total mass of the detector is 0.98 kton. The FD has 484 $8m$ wide octagonal planes and has a total mass of 5.4kton.

In both detectors scintillator planes are comprised of 4.1cm wide strips. The strips are oriented at 45deg with respect to the vertical axis. Consecutive planes have scintillator strips at 90deg. The light from the scintillator is transported to multi-anode photomultiplier tubes via embedded wavelength shifting fibers.

The charged current (CC) and neutral current (NC) events look very different in the MINOS detectors. The typical CC ν_μ event has a long muon track accompanied by a short hadronic shower near the event vertex. The ν_e CC events are characterized by short and dense electromagnetic showers. The NC events are typically short with diffuse hadronic showers.

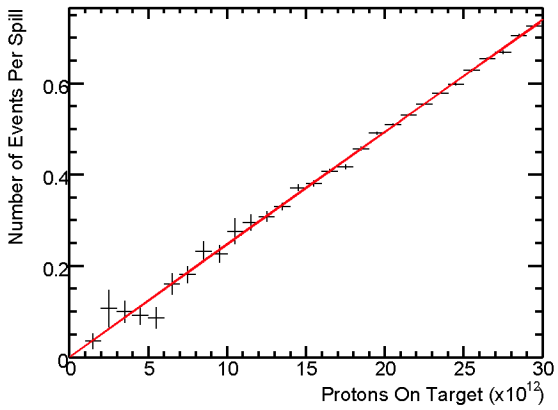

FIGURE 1. Number of selected events in Near Detector per spill as a function of spill intensity. The linearity indicates that there are no biases introduced with higher event rates.

Event reconstruction includes finding and fitting the tracks, and reconstructing the hadronic shower. The reconstructed quantities such as the vertex distribution in the detectors or track angular distributions are well reproduced by the MC. In the ND multiple interactions occur per each beam spill, so timing and spatial information are used to separate individual neutrino interactions. We checked that the intensity of the beam does not introduce any biases in the selected number of events. The linearity shown in Figure 1 indicates that ND is capable of measuring individual neutrino events without any bias due to beam intensity.

For ν_μ CC events, the total reconstructed energy is obtained by summing the reconstructed muon energy and the visible energy, E_{shower}, of the hadronic system. The muon energy is measured either by range or through curvature measurement depending on whether the muon stops in the detector or escapes. Below 10GeV, the hadronic energy resolution was measured to be $56\%/\sqrt{E[GeV]} \oplus 2\%$. The muon energy resolution $\Delta E_\mu / E_\mu$ varies smoothly from 6% at low energies, where most tracks are contained and momentum is measured from range, to 13% at high energies, where curvature is used to measure the momentum.

The ν_μ CC event candidates are preselected in both detectors by requiring that the vertex falls in the fiducial volume ensuring that the hadronic energy of the event is contained within the volume of the detector. The direction of the track is required to be consistent with the neutrino beam direction and the timing of the event has to be

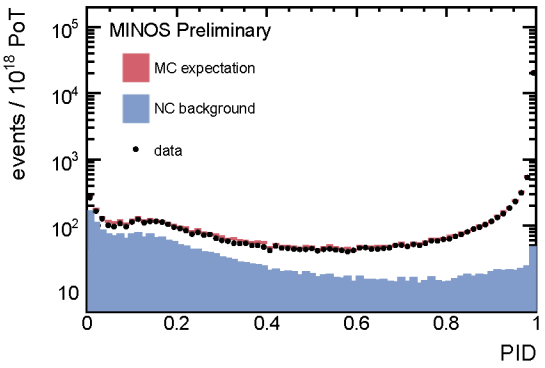

FIGURE 2. Distributions of the CC/NC separation discriminant for ND data. The filled histogram shows the distribution for NC events. CC candidates are selected by requiring that PID>0.85.

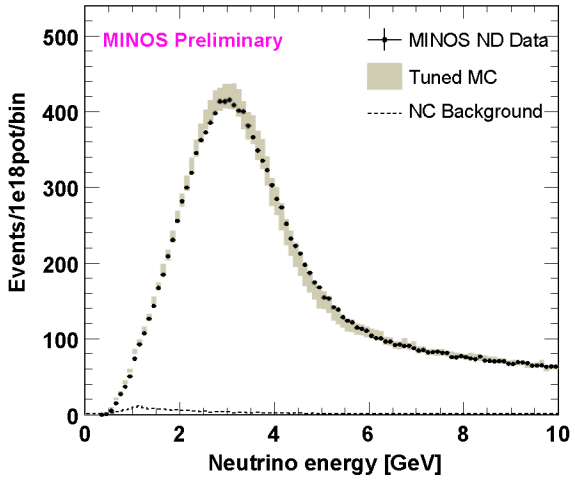

FIGURE 3. Reconstructed neutrino energy spectrum in the Near Detector compared to Monte Carlo prediction. The MC is tuned as described in [8].

consistent with the beam spill time. Subsequently, a multivariate algorithm (PID) is used to separate the ν_μ CC events from the background of NC events. The following variables describing event topology and kinematics are used as input to the PID algorithm: track charge sign, average track pulse height, number of planes with hits on the track, number of planes with hits exclusively on the track, significance of track curvature measurement and reconstructed $y \equiv E_{shower}/E_\nu$. The expected NC background in the selected sample is small and appears in the lowest energy bins. The PID distribution for the ND data is shown in Figure 2. We select events with PID>0.85 in both ND and FD.

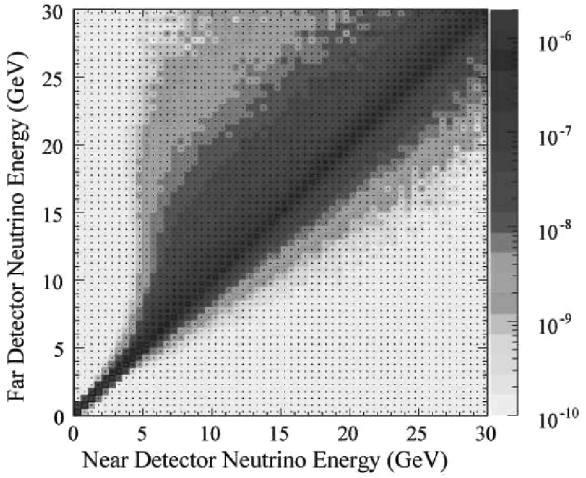

FIGURE 4. The Beam Matrix used to obtain the flux at the Far Detector given the flux at the Near Detector. The matrix element M_{ij} gives the number of neutrinos of energy E_j expected in the FD for every observed neutrino in the ND of energy E_i. The matrix is almost diagonal at lower energies where the focusing peak is.

The analysis presented here uses only ν_μ CC events. The $\bar{\nu}_\mu$ component is separated by requiring that the muon track in the selected event is negative. Figure 3 shows the selected ν_μ CC events below 10GeV along with the MC prediction.[8]

4. OSCILLATION ANALYSIS

To predict the unoscillated FD spectrum the Beam Matrix method [11] is used. The method minimizes the dependence on MC and is less sensitive to mis-modeling of the neutrino flux and neutrino interaction cross sections. The method uses beam simulation to derive the matrix that relates the energy of ν_μs in two detectors via their parent hadrons. The matrix element M_{ij} gives the number of neutrinos of energy E_j expected in the FD for every observed neutrino in the ND of energy E_i. It is calculated using the decay kinematics of secondary hadrons in the beam line. Given the neutrino flux at the ND, the flux at the FD can be obtained using this beam matrix. The beam matrix, shown in Figure 4, is almost diagonal due to the fact that the neutrino parents are focused towards both the ND and FD.

The method consists of three steps. In first step the flux at the ND is extracted. For that it is necessary to correct the reconstructed spectrum for purity and efficiency and divide it by cross sections. In the second step the beam matrix is used on the flux yielding the flux at the FD. In the final step the flux is multiplied with cross sections

TABLE 1. Shifts in oscillation parameters due to various systematic effects. The last row of the table shows the statistical uncertainty for an exposure of $2.5 \times 10^{20} POT$.

Uncertainty	Δm^2 $(10^{-4} eV^2)$	$\sin^2(2\theta)$
Near/Far normalization ($\pm 4\%$)	0.65	<0.005
Abs. hadronic energy scale ($\pm 10\%$)	0.75	<0.005
NC contamination ($\pm 50\%$)	0.10	0.008
All other systematics	0.41	<0.005
Total systematic	1.1	0.008
Statistical error (data)	1.7	0.080

and used in the FD Monte Carlo to create the expected reconstructed neutrino spectrum which is then compared to the data. To first order, dividing with cross sections in the first step cancels with cross section multiplication in the last step making the method insensitive to cross section uncertainties. This happens because the beam matrix is almost diagonal so to first order it commutes with operations involving cross sections.

With an exposure of 2.5×10^{20} protons on target, a total of 738 ± 30 events are expected at the FD in the absence of oscillations. We observe 563 charged-current muon neutrino candidates. The deficit is more significant in low energy region of the spectrum indicating the energy dependence of the deficit. Below 5GeV 198 events are selected, compared to an expected 350 ± 14 events.

Under the assumption that the observed deficit is due to $\nu_\mu \rightarrow \nu_\tau$ oscillations, a maximum likelihood fit is performed to determine the parameters $|\Delta m^2|$ and $\sin^2(2\theta)$. The most significant sources of systematic uncertainty, namely relative FD/ND normalization ($\pm 4\%$), the hadronic shower energy scale ($\pm 10\%$) and the NC background ($\pm 50\%$), are included in the fit as nuisance parameters.

The effects of different systematic uncertainties were evaluated by generating the Monte Carlo sample for ND and FD with a particular systematic shift. A fit to the oscillation parameters $|\Delta m^2|$ and $\sin^2(2\theta)$ was performed and systematic errors on the oscillation parameters were obtained by looking at shifts of the best fit point in the presence of each systematic shift. Table 1 lists the systematic errors in the oscillation parameters. For the current exposure the total error is dominated by the statistical error. It is expected that with future analysis improvements the systematic error will be further reduced.

Figure 5 and 6 show the predicted FD spectrum weighted according to the best-fit oscillation parameter values overlaid on the observed spectrum. The best-fit yields $|\Delta m^2_{23}| = (2.38^{+0.20}_{-0.16}) \times 10^{-3} eV^2$ and $\sin^2(2\theta_{23}) = 1.00_{-0.08}$ with $\chi^2 = 41.2$ for 34 degrees of freedom. Only values of $\sin^2(2\theta) \leq 1$ were considered. The uncertainties represent 68% CL intervals as estimated from

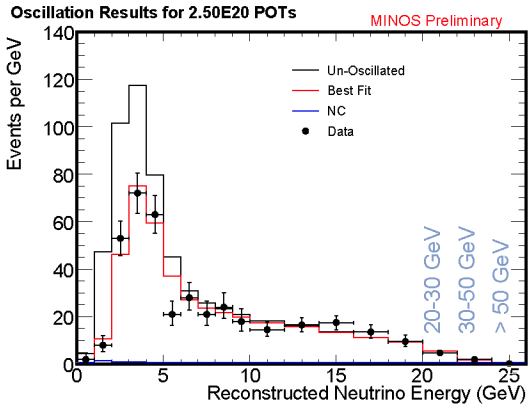

FIGURE 5. The reconstructed ν_μ CC energy spectrum from the Far Detector data compared to predicted unoscillated spectrum and best-fit oscillated spectrum. The expected neutral current background is also shown.

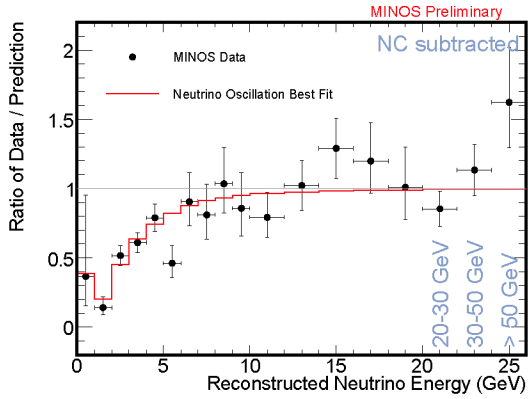

FIGURE 6. The ratio of the observed spectrum to the unoscillated prediction with the best-fit oscillation prediction. The expected neutral current background has been subtracted.

the oscillation parameter values giving an increase in χ^2 of one unit relative to the best-fit value when minimized with respect to all other parameters. The 90% lower limit on $\sin^2(2\theta_{23})$ is found to be 0.84.

Letting the $\sin^2(2\theta)$ assume unphysical values moves the best fit value to $|\Delta m^2_{23}| = 2.26 \times 10^{-3} eV^2$ and $\sin^2(2\theta_{23}) = 1.07$ with $\chi^2 = 40.9$.

The 68% and 90% CL contours in oscillation parameter space are shown in Figure 7. The contours correspond to $\Delta\chi^2 = 2.30$ and 4.61, respectively, relative to the best fit point. We have confirmed the coverage of these confidence intervals using the unified approach of Feldman and Cousins [12].

Figure 8 compares this preliminary result to the first MINOS published result based upon 1.27×10^{20} POT[5]. The allowed region is shifted to lower values of Δm^2. To check that the new result is consistent with the

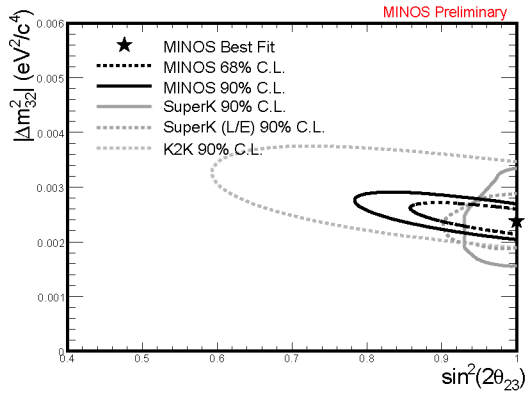

FIGURE 7. Allowed regions in the Δm^2, $\sin^2 2\theta$ plane at 68% and 90% C.L. as determined according to $\Delta\chi^2 = 2.30$ and 4.61, respectively. The best fit point occurs at $\Delta m^2 = 2.38 \times 10^{-3} eV^2/c^4$ and $sin^2 2\theta = 1$. Overlaid are the 90% C.L contours from the Super-Kamiokande zenith angle [1] and L/E analyses [2] and from the K2K experiment [3].

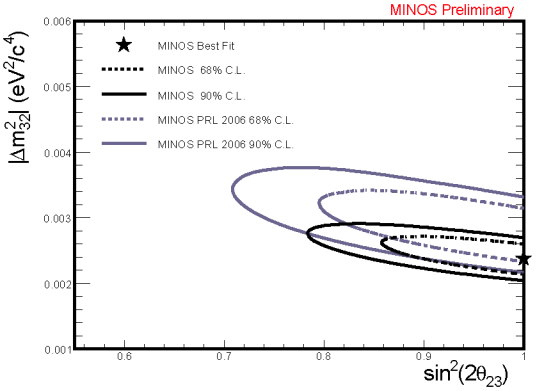

FIGURE 8. The new preliminary contours are compared to the first published MINOS result [5]. The 68% and 90% C.L. curves are determined according to $\Delta\chi^2 = 2.30$ and 4.61, respectively.

old one we separated the data used for the first result and analysed the two data sets independently. Using the data from the first run period yields $\Delta m^2 = (2.50^{+0.24}_{-0.20}) \times 10^{-3} eV^2/c^4$ and the remaining data gives $\Delta m^2 = (2.22^{+0.44}_{-0.22}) \times 10^{-3} eV^2/c^4$. This can be compared to the first MINOS result $\Delta m^2 = (2.74^{+0.44}_{-0.26}) \times 10^{-3} eV^2/c^4$. The shift in Δm^2 for the first run period is in part due to an improved model of neutrino interactions [9, 10] which resulted in the change in the absolute shower energy scale. The change makes a downward systematic shift of $0.06 \times 10^{-3} eV^2/c^4$. The remaining shift in Δm^2 is consistent with a statistical fluctuation due to the increased number of events in the sample caused by improvements mentioned in Section 1.

5. SUMMARY

Here reported is the preliminary result on ν_μ disappearance from the MINOS experiment based on an exposure of 2.5×10^{20} protons on target. A deficit of ν_μ CC events is observed with 6.2σ significance below 10GeV. The systematic errors are under control and well below the current statistical errors. A fit to the $\nu_\mu \rightarrow \nu_\tau$ oscillation hypothesis yields:

$$|\Delta m^2_{23}| = (2.38^{+0.20}_{-0.16}) \times 10^{-3} eV^2 \ \ (68\%\ \text{CL errors})$$

$$\sin^2(2\theta_{23}) > 0.84 \ \ (90\%\ \text{CL})$$

where the uncertainty includes both statistical and systematic sources.

REFERENCES

1. Y. Ashie et al., Phys. Rev. *D 71*, 112005 (2005)
2. Y. Ashie et al., Phys. Rev. Lett *93*, 101801 (2004)
3. M.H. Ahn et al., Phys. Rev. *D 74*, 072003 (2006)
4. M.Sanchez, "Electron Neutrino appearance in the MINOS Experiment", presented at this workshop
5. D.G. Michael et al., Phys. Rev. Lett *97*, 191801 (2006)
6. M. Kordosky and D. Petyt for the MINOS Collaboration, hep-ex/07110769 (2007)
7. R. Brun et al., GEANT Detector Description and Simulation Tool, CERN Program Library, W5013, 1994
8. S.Kopp, "Neutrino Spectra and Uncertainties for MINOS", presented at this workshop
9. NEUGEN version 3.5.0. See H. Gallagher, "The NEUGEN Neutrino Event Generator", Nucl.Phys.Proc.Suppl.112:188-194,2002 as a reference for earlier versions.
10. Proceedings of the 5th International Workshop on Neutrino-Nucleus Interactions in the Few-GeV Region
11. M.Szleper and A.Para, hep-ex/0110001 (2001)
12. G.H.Feldman and R.D.Cousins, Phys.Rev.*D 57*, 3873 (1998)